Environment International Journal

The variability of mass concentrations and source apportionment analysis of equivalent black carbon across urban Europe

Marjan Savadkoohi [a, b], Marco Pandolfi [a], Cristina Reche [a], Jarkko V. Niemi [c], Dennis Mooibroek [d], Gloria Titos [e], David C. Green [f,g], Anja H. Tremper [f], Christoph Hueglin [h], Eleni Liakakou [i], Nikos Mihalopoulos [i], Iasonas Stavroulas [i], Begoña Artiñano [j], Esther Coz [j], Lucas Alados-Arboledas [e], David Beddows [k], Véronique Riffault [l], Joel F. De Brito [l], Susanne Bastian [m], Alexia Baudic [n], Cristina Colombi [o], Francesca Costabile [p], Benjamin Chazeau [q, r], Nicolas Marchand [q], José Luis Gómez-Amo [s], Víctor Estellés [s], Violeta Matos [s], Ed van der Gaag [t], Grégory Gille [u], Krista Luoma [v], Hanna E. Manninen [c], Michael Norman [w], Sanna Silvergren [w], Jean-Eudes Petit [x], Jean-Philippe Putaud [y], Oliver V. Rattigan [z], Hilkka Timonen [aa], Thomas Tuch [bb], Maik Merkel [bb], Kay Weinhold [bb], Stergios Vratolis [cc], Jeni Vasilescu [dd], Olivier Favez [ee], Roy M. Harrison [k, ff], Paolo Laj [gg, hh], Alfred Wiedensohler [bb], Philip K. Hopke [ii], Tuukka Petäjä [hh], Andrés Alastuey [a], Xavier Querol [a]

[a] *Institute of Environmental Assessment and Water Research (IDAEA-CSIC), Barcelona, Spain*

[b] *Department of Mining, Industrial and ICT Engineering (EMIT), Manresa School of Engineering (EPSEM), Universitat Politècnica de Catalunya (UPC), 08242 Manresa, Spain*

[c] *Helsinki Region Environmental Services Authority (HSY), Helsinki, Finland*

[d] *Centre for Environmental Monitoring, National Institute for Public Health and the Environment (RIVM), the Netherlands*

[e] *Andalusian Institute for Earth System Research (IISTA-CEAMA), University of Granada, Granada, Spain*

[f] *MRC Centre for Environment and Health, Environmental Research Group, Imperial College London, UK*

[g] *NIHR HPRU in Environmental Exposures and Health, Imperial College London, UK*

[h] *Laboratory for Air Pollution and Environmental Technology, Swiss Federal Laboratories for Materials Science and Technology (Empa), Duebendorf, Switzerland*

[i] *Institute for Environmental Research & Sustainable Development, National Observatory of Athens, Athens, Greece*

[j] *Centro de Investigaciones Energéticas, Medioambientales y Tecnológicas, Department of Environment, CIEMAT, Madrid, Spain*

[k] *Division of Environmental Health & Risk Management, School of Geography, Earth & Environmental Sciences, University of Birmingham, Edgbaston, Birmingham, United Kingdom*

[l] *IMT Nord Europe, Institut Mines-Télécom, Univ. Lille, Centre for Energy and Environment, Lille, France*

[m] *Saxon State Office for Environment, Agriculture and Geology/Saxon State Department for Agricultural and Environmental Operations, Dresden, Germany*

[n] *AIRPARIF (Ile de France Air Quality Monitoring network), Paris, France*

[o] *Arpa Lombardia, Settore Monitoraggi Ambientali, Unità Operativa Qualità dell'Aria, Milano, Italy*

[p] *Institute of Atmospheric Sciences and Climate-National Research Council, Rome, Italy*

[q] *Aix Marseille Univ., CNRS, LCE, Marseille, France*

[r] *Laboratory of Atmospheric Chemistry, Paul Scherrer Institute, 5232 Villigen, Switzerland*

[s] *Solar Radiation Group. Dept. Earth Physics and Thermodynamics. University of Valencia, Burjassot, Spain*

[t] *DCMR Environmental Protection Agency, Department Air and Energy, Rotterdam, the Netherlands*

[u] *AtmoSud, Regional Network for Air Quality Monitoring of Provence-Alpes-Cote-d'Azur, Marseille, France*

[v] *Institute for Atmospheric and Earth System Research/Physics, Faculty of Science, University of Helsinki, Helsinki, Finland*

[w] *Environment and Health Administration, SLB-analysis, Stockholm, Sweden*

[x] *Laboratoire des Sciences du Climat et de l'Environnement, CEA/Orme des Merisiers, Gif-sur-Yvette, France*

[y] *European Commission, Joint Research Centre (JRC), Ispra, Italy*

[z] *Division of Air Resources, New York State Dept of Environmental Conservation, New York, USA*

[aa] *Atmospheric Composition Research, Finnish Meteorological Institute, Helsinki, Finland*

[bb] *Leibniz Institute for Tropospheric Research (TROPOS), Leipzig, Germany*

[cc] *Environmental Radioactivity Laboratory, Institute of Nuclear & Radiological Sciences & Technology, Energy & Safety, N.C.S.R. "Demokritos", Athens, Greece*

[dd] *National Institute of Research and Development for Optoelectronics INOE 2000, Magurele, Romania*

[ee] *Institut National de l'Environnement Industriel et des Risques (INERIS), Verneuil-en-Halatte, France*

[ff] *Department of Environmental Sciences, Faculty of Meteorology, Environment and Arid Land Agriculture, King Abdulaziz University, Jeddah, Saudi Arabia*

[gg] *Univ. Grenoble, CNRS, IRD, IGE, 38000, Grenoble, France*

[hh] *Institute for Atmospheric and Earth System Research/Physics (INAR), Faculty of Science, University of Helsinki, Helsinki, Finland*

[ii] *Department of Public Health Sciences, University of Rochester School of Medicine & Dentistry, Rochester, NY, USA*

*** Corresponding authors.**

E-mail address: *marjan.savadkoohi@idaea.csic.es (M. Savadkoohi), marco.pandolfi@idaea.csic.es (M. Pandolfi)*

Summary of the number of pages, tables, and figures:

Number of pages: 18

Number of Tables: 6

Number of Figures: 6

Table S1. List of the 50 monitoring sites that have supplied eBC mass concentration datasets to this study. The table includes detailed information such as the location of each site, the type of site (UB, Urban Background; TR, Traffic; SUB, Suburban Background; RG, Regional Background), the instrument used for measurements, and specific measurement details including altitude and measurement height. The table presents eBC mass concentration and absorption coefficient (b_{abs}) data from various countries, including Finland (FI), Sweden (SE), United Kingdom (UK), Netherlands (NL), France (FR), Spain (ES), Greece (GR), Romania (RO), Germany (DE), Switzerland (CH), and Italy (IT). The eBC mass concentration values are reported in units of μg m^{-3}. The type of data received indicates whether it is compiled as eBC mass concentration or absorption coefficient. The data is categorized as either hourly averaged (supplied by data providers) or raw data, which refers to raw data obtained directly from the instrument with original time resolution. Level 2 data refers to quality-checked hourly averaged data that has been downloaded from the EBAS database.

Region	Site	City Country	Type	Acronym	Coordinates	Altitude (m.a.s.l.)	Instrument	measurement height [m]	Data received	Data source	Data coverage
Northern Europe	Mannerheimintie	Helsinki-FI	TR	HEL_TR1	60.1697, 24.939	10	MAAP	4	eBC	RI-URBAN (Hourly)	01/01/2011- 12/31/2019
	Mäkelänkatu	Helsinki-FI	TR	HEL_TR2	60.196, 24.952	25	MAAP	4	eBC	RI-URBAN (Hourly)	01/30/2015- 12/31/2019
	Töölöntulli	Helsinki-FI	TR	HEL_TR3	60.190, 24.916	24	MAAP	4	eBC	RI-URBAN (Hourly)	11/01/2010- 30/12/2015
	Kehä I	Helsinki-FI	TR	HEL_TR4	60.241, 25.025	15	MAAP	4	eBC	RI-URBAN (Hourly)	01/01/2012- 12/28/2012
	Tikkurila	Helsinki-FI	TR	HEL_TR5	60.289, 25.039	22	MAAP	4	eBC	RI-URBAN (Hourly)	Years 2014, 2016 & 2018
	Leppävaara	Helsinki-FI	TR	HEL_TR6	60.220, 24.811	13	MAAP	4	eBC	RI-URBAN (Hourly)	Years 2015 & 2017
	Kallio	Helsinki-FI	UB	HEL_UB	60.1872, 24.950	18	MAAP	4	eBC	RI-URBAN (Hourly)	01/04/2012-12/31/2019
	Rekola	Helsinki-FI	SUB	HEL_SUB1	60.331, 25.075	29	AE33	4	7 (λ) eBC	RI-URBAN (Hourly)	05/01/2017-31/05/2017
	Itä-Hakkila	Helsinki-FI	SUB	HEL_SUB2	60.291, 25.112	41	AE33	4	7 (λ) eBC	RI-URBAN (Hourly)	03/01/2018-23/10/2018
	Pirkkola	Helsinki-FI	SUB	HEL_SUB3	60.234, 24.922	27	AE33	4	7 (λ) eBC	RI-URBAN (Hourly)	31/12/2018-31/12/2019
	SMEAR II	Hyytiälä, FI	RB	SMR_RB	61.847, 24.295	181	AE33	4	7 (λ) eBC & 7 (λ) babs	RI-URBAN (Hourly)	15/03/2018-31/12/2021
						181	AE31	4	7 (λ) eBC & 7 (λ) babs	RI-URBAN (Hourly)	31/05/2006-17/11/2017
						181	MAAP	4	eBC	RI-URBAN (Hourly)	18/06/2013-09/05/2021
	Hornsgatan 108	Stockholm-SE	TR	STH_TR	59.3171, 18.048	25	AE33	4	7 (λ) eBC	RI-URBAN (Hourly)	14/10/2014-31/12/2019

						25	MAAP	4	eBC	RI-URBAN (Hourly)	04/11/2015-05/12/2016
	Torkel Knutssonsgatan	Stockholm-SE	UB	STH_UB	59.316, 18.057	48	AE33	24	7 (λ) eBC	RI-URBAN (Hourly)	10/14/2014 -12/31/2019
						48	MAAP	24	eBC	RI-URBAN (Hourly)	10/02/2014- 11/3/2015
North-Western Europe	BAQS	Birmingham-UK	UB	BIR_UB	52.455, -1.928	143	AE33	3	7 (λ) eBC	RI-URBAN (Hourly)	03/19/2019- 2/23/2022
	North Kensington	London-UK	UB	LND_UB	51.521, -0.213	27	AE22	2.8	2 (λ) eBC	RI-URBAN (Hourly)	01/01/2009- 11/07/2019
						27	AE33	2.8	7 (λ) eBC	RI-URBAN (Hourly)	01/01/2020- 01/01/2022
	Marylebone Road	London-UK	TR	LND_TR	51.522, -0.1546	35	AE22	3	2 (λ) eBC	RI-URBAN (Hourly)	16/03/2009-31/12/2019
						35	AE33	3	7 (λ) eBC	RI-URBAN (Hourly)	01/24/2020- 01/01/2022
Western Europe	Winkelhorst	Enschede-NL	UB	NLD_UB1	52.234, 6.919	38	MAAP	3	eBC	RI-URBAN (Hourly)	04/29/2015-12/31/2021
	Nijensteinheerd	Groningen-NL	UB	NLD_UB2	53.246, 53.246	-1	MAAP	3	eBC	RI-URBAN (Hourly)	05/04/2015-12/31/2021
	Jamboreepad	Heerlen-NL	UB	NLD_UB3	50.900, 5.986	98	MAAP	3	eBC	RI-URBAN (Hourly)	04/09/2015- 12/31/2021
	Ruyterstraat	Nijmegen-NL	UB	NLD_UB4	51.838, 5.856	28	MAAP	3	eBC	RI-URBAN (Hourly)	04/30/2015- 12/31/2021
	Europalaan	Veldhoven-NL	UB	NLD_UB5	51.407, 5.393	22	MAAP	3	eBC	RI-URBAN (Hourly)	05/21/2015- 12/31/2021
	Noordbrabantlaan	Eindhoven-NL	TR	NLD_TR1	51.444, 5.444	18	MAAP	3	eBC	RI-URBAN (Hourly)	28/04/2015-31/12/2021
	Graafseweg	Nijmegen-NL	TR	NLD_TR2	51.841, 5.857	28	MAAP	3	eBC	RI-URBAN (Hourly)	26/05/2015-31/12/2021
	NL01487 (RPW)	Rotterdam-NL	TR	NLD_TR3	51.891, 4.481	2	MAAP	4	eBC	RI-URBAN (Hourly)	01/01/2010-31/12/2021
	NL01488 (RZW)	Rotterdam-NL	UB	NLD_UB6	51.894, 4.4876	0	MAAP	4	eBC	RI-URBAN (Hourly)	01/01/2010- 12/31/2021

	NL01492 (RDM)	Rotterdam-NL	TR	NLD_TR4	51.914, 4.48	-1	MAAP	4	eBC	RI-URBAN (Hourly)	01/07/2007-31/12/2021
	Paris-13	Paris-FR	UB	PAR_UB	48.828, 2.359	57	AE33	2.3	7 (λ) eBC	RI-URBAN (Hourly)	01/01/2016-12/31/2019
	Haussmann	Paris-FR	TR	PAR_TR	48.874, 2.330	42	AE33	3.8	7 (λ) eBC	RI-URBAN (Hourly)	01/01/2016- 12/29/2019
	ATOLL	Lille-FR	SUB	LIL_SUB	50.611, 3.1403	70	AE33	20	7 (λ) eBC	RI-URBAN Raw data	01/01/2017-31/12/2019
	SIRTA	Paris-FR	SUB	PAR_SUB	48.7086, 2.1588	162	AE33	15	7 (λ) eBC	RI-URBAN (Hourly)	01/01/2014-30/12/2020
South-western Europe	Longchamp	Marseille-FR	UB	MAR_UB	43.305, 5.394	73	AE33	3	7 (λ) eBC	RI-URBAN (Hourly)	01/01/2017-12/31/2019
	Palau Reial	Barcelona-ES	UB	BCN_UB	41.387, 2.115	80	AE33	4	7 (λ) eBC & 7 babs	RI-URBAN (Hourly)	04/03/2015-9/20/2020
						64	MAAP	4	eBC	RI-URBAN (Hourly)	01/13/2009- 3/31/2021
	UGR	Granada-ES	UB	GRA_UB	37.18, -3.58	680	AE33	15	7 (λ) eBC	RI-URBAN (Hourly)	01/01/2014-12/31/2019
						680	MAAP	15	eBC	RI-URBAN (Hourly)	01/01/2006-31/12/2020
	CIEMAT	Madrid-ES	UB	MAD_UB	40.456, -3.725	669	AE33	4	7 (λ) eBC	RI-URBAN (Hourly)	14/01/2013-31/12/2019
	Burjassot	Valencia-ES	UB	VLC_UB	39.51, - 0.42	40	AE31	15	7 (λ) eBC & 7 babs	RI-URBAN (Hourly)	01/09/2017-12/7/2020
South-Eastern Europe	Thissio	Athens-GR	UB	ATH_UB	37.973, 23.718	105	AE33	4	7 (λ) eBC & 7 ATN	RI-URBAN (Hourly)	01/01/2017-12/31/2019
	Demokritos	Athens-GR	SUB	ATH_SUB	37.99, 23.82	270	AE33	6	7 (λ) babs	RI-URBAN (Hourly)	11/01/2017-31/12/2019
Eastern Europe	INO	Bucharest-RO	SUB	BU_SUB	44.348, 26.029	93	AE33	15	7 (λ) eBC	RI-URBAN Raw data	27/02/2014-11/01/2022
Central Europe	Winckelmannstrasse	Dresden-DE	UB	DDW_UB	51.036, 13.730	120	MAAP	3.5	eBC	RI-URBAN (Hourly)	01/01/2017-12/31/2019
	Nord	Dresden-DE	TR	DDN_TR	51.087, 13.7630	112	MAAP	4	eBC	RI-URBAN (Hourly)	01/01/2017-31/12/2019

	TROPOS	Leipzig-DE	UB	LEJ_UB	51.352, 12.434	113	MAAP	4	babs_670nm	EBAS Level 2	01/01/2009-12/31/2020
	Mitte	Leipzig-DE	TR	LEJ_TR1	51.344, 12.377	111	MAAP	4	babs_670nm	EBAS Level 2	04/01/2017-26/12/2019
	Eisenbahnstrasse	Leipzig-DE	TR	LEJ_TR2	51.345, 12.406	120	MAAP	4	babs_670nm	EBAS Level 2	17/01/2009-31/12/2020
	Bollwerk	Bern-CH	UB/TR	BER_UB	46.951, 7.440	536	AE33	4	7 (λ) babs	RI-URBAN (Hourly)	01/01/2015- 12/31/2021
	Università	Lugano-CH	UB	LUG_UB	46.011, 8.9572	287	AE33 & MAAP	3	babs 880nm	RI-URBAN (Hourly)	11/03/2021- 12/31/2021
						287		3	babs 670 nm	RI-URBAN (Hourly)	11/03/2021- 12/31/2021
	Kaserne	Zurich-CH	UB	ZUR_UB	47.3775, 8.5305	409	AE33	3	7 (λ) babs	RI-URBAN (Hourly)	01/01/2012- 12/31/2021
	Pascal	Milan-IT	UB	MLN_UB	45.464, 9.188	118	AE33	2.5	7 (λ) eBC & 7 babs	RI-URBAN (Hourly)	06/08/2018-11/04/2019
						118	MAAP	2.5	eBC	RI-URBAN (Hourly)	06/02/2013-21/11/2021
	Senato	Milan-IT	TR	MLN_TR1	45.464, 9.188	121	AE33	2.5	7 (λ) eBC	RI-URBAN (Hourly)	12/06/2019-22/11/2021
	Marche	Milan-IT	TR	MLN_TR2	45.464, 9.188	129	AE33	2.5	7 (λ) eBC	RI-URBAN (Hourly)	12/06/2019-22/11/2021
	Ispra	IPR_IT	RB	IPR_RB	45.8, 8.633	209	EBAS MAAP	9	babs_670nm	EBAS Level 2	16/09/2008-31/12/2020

Table S2. eBC mass concentration statistics (minimum, maximum, mean, data coverage%, and seasonal mean concentrations) of monitoring sites in µg m^{-3} between 2017-2019. UB, Urban Background; TR, Traffic; SUB, Suburban Background; RG, Regional Background.

Region	Site	Instrument	Min	Max	Mean	Data Coverage%	Autumn (SON)	Winter (DJF)	Spring (MAM)	Summer (JJA)
Northern Europe	HEL (TR1)	MAAP	0.02	8.38	0.68± 0.56	87.4	0.71	0.71	0.65	0.65
	HEL (TR2)	MAAP	0.01	16.37	0.97± 0.85	98.5	1.01	0.93	0.9	1.03
	HEL (TR5)	MAAP	0.02	9.74	0.81± 0.88	24.2	0.78	0.83	0.77	0.85
	HEL (TR6)	MAAP	0.01	10.52	0.67± 0.68	65.3	0.76	0.78	0.51	0.63
	HEL (UB1)	MAAP	0.01	7.14	0.45± 0.42	98.6	0.46	0.58	0.4	0.34
	HEL (SUB1)	AE33	0.03	26.95	0.96± 1.92					
	HEL (SUB2)	AE33	0.01	17.58	0.96± 1.20	98.8	0.99	1.24	1.02	0.60
	HEL (SUB3)	AE33	0.01	30.31	0.74± 1.30					
	SMR (RB)	AE31	0	3.62	0.17± 0.21	68.1	0.2	0.27	0.11	0.14
	SMR (RB)	AE33	0	3.09	0.28± 0.29	87.3	0.31	0.25	0.29	0.26
	SMR (RB)	MAAP	0	4.55	0.19± 0.22	88.9	0.21	0.26	0.17	0.14
	STH (TR)	AE33	0.03	30.4	0.88± 0.68	91	0.92	0.77	0.96	0.87
	STH (UB)	AE33	0.01	4.72	0.31± 0.29	88.1	0.33	0.33	0.35	0.24
North-Western Europe	BIR (UB)	AE33	0.02	14.96	0.76± 0.82	97.4	0.9	0.87	0.75	0.59
	LND (UB)	AE22	0	13.5	0.84± 0.92	95.3	0.92	1.16	0.71	0.6
	LND (TR)	AE22	0.1	18.3	2.94± 2.24	96.6	3.13	3.03	2.53	3.01
Western Europe	NLD (UB1)	MAAP	-0.5	11.2	0.74± 0.78	98.5	0.82	1.1	0.62	0.41
	NLD (UB2)	MAAP	0	24.64	0.57± 0.74	97.8	0.58	0.88	0.48	0.33
	NLD (UB3)	MAAP	0	10.41	0.85± 0.88	99.5	0.9	1.12	0.78	0.6
	NLD (UB4)	MAAP	0	9.89	0.88± 0.75	98.8	0.96	1.17	0.77	0.62
	NLD (UB5)	MAAP	0	15.82	0.96± 0.93	99	1.06	1.34	0.83	0.61
	NLD (UB6)	MAAP	0	11.63	0.90± 0.78	98.3	0.98	1.2	0.79	0.63
	NLD (TR1)	MAAP	0.03	11.19	1.37± 10.3	99	1.57	1.64	1.23	1.06
	NLD (TR2)	MAAP	0	15.66	1.53± 1.12	98.7	1.58	1.7	1.46	1.37
	NLD (TR3)	MAAP	0	11.12	1.67± 1.23	98.1	1.89	1.98	1.51	1.3
	NLD (TR4)	MAAP	0	12.28	1.26± 0.99	97.8	1.36	1.59	1.17	0.93
	PAR (UB)	AE33	0.07	18.49	1.46± 1.43	93.3	1.72	1.71	1.25	1.14
	PAR (TR)	AE33	0.11	18.68	2.48± 1.72	96.7	2.78	2.82	2.24	2.13
	LIL (SUB)	AE33	0.03	35.25	1.01± 1.24	62.9	1.17	1.2	0.94	0.72
	PAR (SUB)	AE33	0.01	13.32	0.64± 0.70	95.4	0.68	0.76	0.57	0.53
South-Western Europe	MAR (UB)	AE33	0.06	27	1.61± 1.46	90.8	1.72	2.15	1.22	1.38
	BCN (UB)	AE33	0.04	20.85	1.51± 1.53	52.9	1.62	1.68	1.34	1.37
	BCN (UB)	MAAP	0	23.1	1.30± 1.26	92.1	1.35	1.36	1.26	1.24

	GRA (UB)	AE33	0.06	17.67	2.08± 2.04	66.2	2.31	2.92	1.48	1.48
	GRA (UB)	MAAP	-0.15	25.46	1.95± 2.00	91.9	2.23	2.92	1.3	1.37
	MAD (UB)	AE33	0	79.11	1.35± 1.83	69	1.47	2.4	0.89	0.82
	VAL (UB)	AE31	0	17.84	1.48± 1.34	48.6	1.68	1.73	1.09	1.1
South-Eastern Europe	ATH (UB)	AE33	0.06	32.66	1.76± 2.29	96.1	1.81	2.5	1.49	1.24
	ATH (SUB)	AE33	0	9.5	0.82± 0.55	83.8	0.84	0.86	0.83	0.78
Eastern Europe	BUC (SUB)	AE33	0	91.32	2.13± 3.05	48.2	1.91	2.54	2.99	1.25
Central Europe	DDW (UB)	MAAP	0.05	9.21	0.68± 0.66	99.8	0.78	0.89	0.62	0.43
	DDN (TR)	MAAP	0.05	11.15	1.05± 0.78	99.8	1.13	1.32	0.95	0.8
	LEJ (UB)	MAAP	0.02	13.23	0.92± 1.03	96.4	1.09	1.26	0.84	0.54
	LEJ (TR1)	MAAP	0	18.41	1.82± 1.35	98.3	1.89	2.14	1.75	1.47
	LEJ (TR2)	MAAP	0.01	16.7	1.52± 1.22	75.7	1.35	1.96	1.41	1.44
	Bern (UB/TR)	AE33	0.03	12.99	1.07± 0.79	96.5	1.12	1.35	0.93	0.88
	ZUR (UB)	AE33	0	27.68	0.79± 0.69	99.5	0.97	0.95	0.63	0.61
	LUG (UB)	MAAP	0	4.91	0.59± 0.52	99.6	0.45	0.72	0.47	0.20
	MLN (UB)	AE33	0.01	18.61	3.15±2.90	58.1	2.45	5.01	2.32	1.34
	MLN (UB)	MAAP	0.02	19.11	2.55± 2.50	100	2.84	4.67	1.65	1.1
	MLN (TR1)	AE33	0.13	12.74	2.02± 1.47	84.1	2.48	3.47	…	1.33
	MLN (TR2)	AE33	0.14	17.86	3.37± 2.35	76.6	4.5	5.16	2	2.3
	IPR (RB)	MAAP	0	11.85	1.45± 1.55	87.7	1.47	2.79	0.89	0.63

Table S3. Aethalometer model statistics (PM size, mean relative contribution%, mass concentrations ug m^{-3} at 95% confidence interval (CI), and seasonal mean relative contribution%) using AAE_T= 1, AAE_{RC}= 2, Sandradewi et al. (2008) during 2017-2019.

Region	Site name	PM size	Mean relative % eBC_T	Mean relative % eBC_{RC}	**eBC_T ug m^{-3}**	**eBC_{RC} ug m^{-3}**	eBC_T mean relative % summer (JJA)	eBC_T mean relative % winter (DJF)	eBC_{RC} mean relative % summer (JJA)	eBC_{RC} mean relative % winter (DJF)
Northern	HEL_SUB2	PM1	65.65	34.35	0.61; 95% CI [0.10, 1.79]	0.35; 95% CI [0.04, 1.14]				
	HEL_SUB3	PM1	68.68	31.32	0.49; 95% CI [0.06, 1.53]	0.24; 95% CI [0.02, 0.76]	71.26	64.99	28.74	35.00
	HEL_SUB1	PM1	69.47	30.50	0.63; 95% CI [0.07, 1.90]	0.33; 95% CI [0.02, 1.09]				
	SMR_RB	PM10	89.17	10.83	0.25; 95% CI [0.04, 0.73]	0.03; 95% CI [0.00, 0.14]	93.79	88.35	6.21	11.65
	STH-TR	PM1	86.66	13.34	0.77; 95% CI [0.14, 1.91]	0.11; 95% CI [0.00, 0.38]	90.82	80.03	9.18	19.97
	STH-UB	PM1	75.41	24.59	0.22; 95% CI [0.05, 0.60]	0.08; 95% CI [0.00, 0.30]	83.44	68.76	16.56	31.24
Western	PAR_TR	PM2.5	87.71	12.29	2.17; 95% CI [0.55, 5.06]	0.31; 95% CI [0.00, 0.99]	92.65	81.27	7.35	18.73
	PAR-UB	PM2.5	85.82	14.18	1.23; 95% CI [0.27, 3.31]	0.22; 95% CI [0.00, 0.8]	92.82	76.01	7.18	23.99
	PAR-SUB	PM1	71.41	28.59	0.46; 95% CI [0.04, 1.44]	0.18; 95% CI [0.01, 0.62]	85.18	56.08	14.82	43.92
	LIL_SUB	PM1	69.40	30.60	0.68; 95% CI [0.14, 1.76]	0.33; 95% CI [0.04, 1.01]	74.71	63.17	25.29	36.83
North Western	BIR_UB	PM2.5	74.45	25.55	0.57; 95% CI [0.10, 1.58]	0.19; 95% CI [0.04, 0.56]	76.64	68.95	23.36	31.05
South Western	BCN_UB	PM10	84.09	15.91	1.29; 95% CI [0.21, 3.72]	0.22; 95% CI [0.00, 0.69]	92.73	75.76	7.27	24.04
	GRA_UB	Total	70.18	29.82	1.45; 95% CI [0.28, 4.41]	0.63; 95% CI [0.09, 2.03]	76.16	62.66	23.84	37.34
	MAD_UB	PM10	82.90	17.10	1.12; 95% CI [0.13, 3.84]	0.23; 95% CI [0.00, 0.88]	83.33	78.14	16.67	21.86
	MAR_UB	PM2.5	80.23	19.77	1.26; 95% CI [0.29, 3.28]	0.35; 95% CI [0.02, 1.18]	86.11	71.24	13.89	28.76
South Eastern	ATH_SUB	PM10	75.73	24.27	0.62; 95% CI [0.19, 1.48]	0.20; 95% CI [0.02, 0.52]	81.24	65.54	18.76	34.46
	ATH_UB	PM10	69.16	30.84	1.15; 95% CI [0.20, 3.77]	0.60; 95% CI [0.07, 2.06]	74.10	59.22	25.90	40.78
Eastern	BUC_SUB	PM10	61.43	38.57	1.35; 95% CI [0.17, 4.24]	0.77; 95% CI [0.06, 2.60]	76.38	50.34	23.62	49.66
Central	BER_UB	PM2.5	72.86	27.14	0.78; 95% CI [0.17, 1.93]	0.28; 95% CI [0.04, 0.79]	78.39	68.70	21.61	31.30
	ZUR_UB	PM2.5	75.34	24.66	0.59; 95% CI [0.10, 1.54]	0.20; 95% CI [0.03,0.59]	80.89	68.64	19.11	31.36
	MLN_TR1	PM10	77.59	22.41	1.50; 95% CI [0.45, 3.41]	0.53; 95% CI [0.07, 1.88]	84.00	64.89	16.00	35.11
	MLN_TR2	PM10	82.15	17.85	2.68; 95% CI [0.75, 6.11]	0.69; 95% CI [0.07, 2.34]	87.70	68.98	12.30	31.02
	MLN_UB	PM10	74.38	25.62	2.21; 95% CI [0.37, 6.41]	0.94; 95% CI [0.01, 3.29]	85.51	61.35	14.49	38.65

Table S4. Aethalometer model statistics (PM size, mean relative contribution%, mass concentrations ug m^{-3} at 95% confidence interval (CI), and seasonal mean relative contribution%) using AAE_T= 0.90, AAE_{RC}= 1.68, Zotter et al. (2017) during 2017-2019.

Region	Site name	PM size	Mean relative % eBC_T	Mean relative % eBC_{RC}	**eBC_T ug m-3**	**eBC_{RC} ug m-3**	eBC_T mean relative % summer (JJA)	eBC_T mean relative % winter (DJF)	eBC_{RC} mean relative % summer (JJA)	eBC_{RC} mean relative % winter (DJF)
Northern	HEL_SUB2	PM1	46.51	53.49	0.42; 95% CI [0.06, 1.23]	0.54; 95% CI [0.07, 1.72]	53.56	45.68	46.43	54.32
	HEL_SUB3	PM1	50.46	49.54	0.36; 95% CI [0.04, 1.09]	0.38; 95% CI [0.04, 1.19]				
	HEL_SUB1	PM1	51.22	48.78	0.45; 95% CI [0.05, 1.40]	0.51; 95% CI [0.05, 1.66]				
	SMR_RB	PM10	78.50	21.50	0.22; 95% CI [0.03, 0.66]	0.06; 95% CI [0.00, 0.25]	86.91	76.29	13.09	23.71
	STH-TR	PM1	72.66	27.34	0.65; 95% CI [0.11, 1.66]	0.23; 95% CI [0.00, 0.65]	76.98	64.75	23.02	35.25
	STH-UB	PM1	58.35	41.65	0.17; 95% CI [0.03, 0.45]	0.14; 95% CI [0.02, 0.46]	67.81	50.50	32.19	49.50
Western	PAR_TR	PM2.5	72.35	27.65	1.79; 95% CI [0.44, 4.21]	0.69; 95% CI [0.13, 1.80]	78.05	65.01	21.95	34.99
	PAR-UB	PM2.5	70.38	29.62	1.01; 95% CI [0.22, 2.72]	0.45; 95% CI [0.06, 1.39]	78.78	58.85	21.22	41.15
	PAR-SUB	PM1	52.84	47.16	0.34; 95% CI [0.01, 1.12]	0.29; 95% CI [0.03, 0.96]	69.68	33.69	30.32	66.31
	LIL_SUB	PM1	50.92	49.08	0.49; 95% CI [0.09, 1.30]	0.52; 95% CI [0.08, 1.55]	57.49	43.26	42.51	56.74
North Western	BIR_UB	PM2.5	57.36	42.64	0.44; 95% CI [0.08, 1.23]	0.32; 95% CI [0.07, 0.91]	59.95	50.76	38.38	50.11
South Western	BCN_UB	PM10	68.82	31.18	1.06; 95% CI [0.16, 3.09]	0.45; 95% CI [0.05, 1.34]	79.41	58.80	20.59	41.20
	GRA_UB	Total	51.97	48.03	0.98; 95% CI [0.19, 2.78]	1.10; 95% CI [0.15, 3.75]	59.47	42.48	40.53	57.52
	MAD_UB	PM10	67.24	32.76	0.91; 95% CI [0.10, 3.13]	0.44; 95% CI [0.04, 1.62]	67.66	61.92	32.34	38.08
	MAR_UB	PM2.5	63.70	36.30	0.99; 95% CI [0.21, 2.57]	0.62; 95% CI [0.11, 1.93]	70.56	52.95	29.44	47.05
South Eastern	ATH_SUB	PM10	58.63	41.37	0.48; 95% CI [0.12, 1.19]	0.34; 95% CI [0.08, 0.83]	65.27	46.16	34.73	53.84
	ATH_UB	PM10	50.72	49.28	0.81; 95% CI [0.12, 2.65]	0.95; 95% CI [0.12, 3.19]	57.03	37.92	42.97	62.08
Eastern	BUC_SUB	PM10	40.55	59.45	0.93; 95% CI [0.00, 2.98]	1.20; 95% CI [0.16, 3.95]	59.65	25.87	40.35	74.13
Central	BER_UB	PM2.5	54.97	45.03	0.59; 95% CI [0.11, 1.51]	0.48; 95% CI [0.10, 1.23]	61.62	49.89	38.38	50.11
	ZUR_UB	PM2.5	58.29	41.71	0.45; 95% CI [0.07, 1.19]	0.34; 95% CI [0.06, 0.95]	64.66	50.50	35.34	49.50
	MLN_TR1	PM10	60.68	39.32	1.14; 95% CI [0.34, 2.55]	0.88; 95% CI [0.18, 2.88]	68.31	45.28	31.69	54.72
	MLN_TR2	PM10	65.90	34.10	2.12; 95% CI [0.60, 4.81]	1.25; 95% CI [0.25, 3.69]	72.26	50.66	27.74	49.34
	MLN_UB	PM10	56.99	42.95	1.62; 95% CI [0.28, 4.88]	1.52; 95% CI [0.10, 5.07]	70.68	40.92	29.32	59.08

Table S5. Results of the Theil-Sen nonparametric estimator of the slope with Mann-Kendall tests computed throughout the year (annual) for stations providing more than 9 years of eBC mass concentration with 75% valid data and the common period 2012-2020. (CI): 95% confidence intervals computed by bootstrapping the data. The statistically significant (ss) trends of each site are represented by *** for *p*-value < 0.001, ** for *p*-value < 0.01, * for *p*-value < 0.05, + for *p*-value < 0.1, and ns for not significant.

Site	Slope > 9 years of data [95% CI range] % yr^{-1}	*P*-value > 9 years of data	Slope 2012-2020 [95% CI range] % yr^{-1}	*P*-value 2012-2020
BCN_UB	-4.69 [-4.99; -4.30]	0.00	-5.37 [-6.27; -4.33]	0.00
GRA_UB	-2.80 [-3.15; -2.45]	0.00	-2.41 [-3.35; -1.40]	0.00
LND_UB	-5.82 [-6.44; -4.86]	0.00	-8.32 [-9.52; -7.40]	0.00
LEJ_UB	-3.43 [-4.28; -2.60]	0.00	-3.60 [-5.02; -2.01]	0.00
NLD_UB6	-4.75 [-5.27; -4.21]	0.00	-4.79 [-5.68; -3.89]	0.00
ZUR_UB	-1.66 [-3.73; 0.44]	0.11	-10.00 [-2.85; 2.43]	0.91
LND_TR	-8.38 [-8.40; -7.92]	0.00	-10.45 [-10.87; -9.92]	0.00
LEJ_TR2	-4.06 [-4.64; -3.32]	0.00	-3.30 [-4.25; -2.16]	0.00
NLD_TR3	-5.69 [-6.05; -5.32]	0.00	-6.06 [-6.60; -5.41]	0.00
NLD_TR4	-4.65 [-4.93; -4.24]	0.00	-5.42 [-5.93; -4.65]	0.00
PAR_SUB	-5.68 [-6.69; -4.55]	0.00	-5.92 [-7.15; -4.56]	0.00
IPR_RB	-3.57 [-4.06; -3.07]	0.00	-3.28 [-4.26; -2.34]	0.00
SMR_RB	-3.87 [-5.02; -2.37]	0.00	-6.36 [-8.14; -3.66]	0.00

Table S6. Results of the piecewise linear regression computed throughout the year (annual) for stations providing more than 9 years of eBC mass concentration with 75% valid data. No: the number of breakpoints; RMSE: root mean squared error expressed in µg m^{-3}; MAE: mean absolute error expressed in µg m^{-3}.

Site	Breakpoint No.	Date of Breakpoint	Standard error (uncertainty)	Slope	Adj. R2	RMSE	MAE
BCN_UB	1	2/1/2019	8.74	-0.008	0.54	0.34	0.24
GRA_UB	1	1/1/2009	5.75	-0.007	0.5	0.38	0.25
LND_UB	1	7/1/2009	3.10	-0.008	0.43	0.37	0.26
LEJ_UB	1	4/1/2015	30.57	-0.005	0.2	0.43	0.28
NLD_UB6	1	6/1/2013	10.65	-0.006	0.49	0.27	0.18
ZUR_UB	1	1/1/2015	5.69	-0.001	0.19	0.31	0.18
LND_TR	1	8/1/2011	6.37	-0.071	0.86	1.11	0.82
LEJ_TR2	1	5/1/2012	11.04	-0.008	0.42	0.43	0.3
NLD_TR3	1	7/1/2012	10.65	-0.015	0.75	0.38	0.27
NLD_TR4	1	6/1/2014	21.67	-0.010	0.66	0.35	0.25
PAR_SUB	1	2/1/2013	6..50	-0.005	0.3	0.28	0.19
IPR_RB	1	7/1/2014	19.11	-0.008	0.29	0.53	0.35
SMR_RB	1	12/1/2010	10.11	-0.001	0.22	0.11	0.08

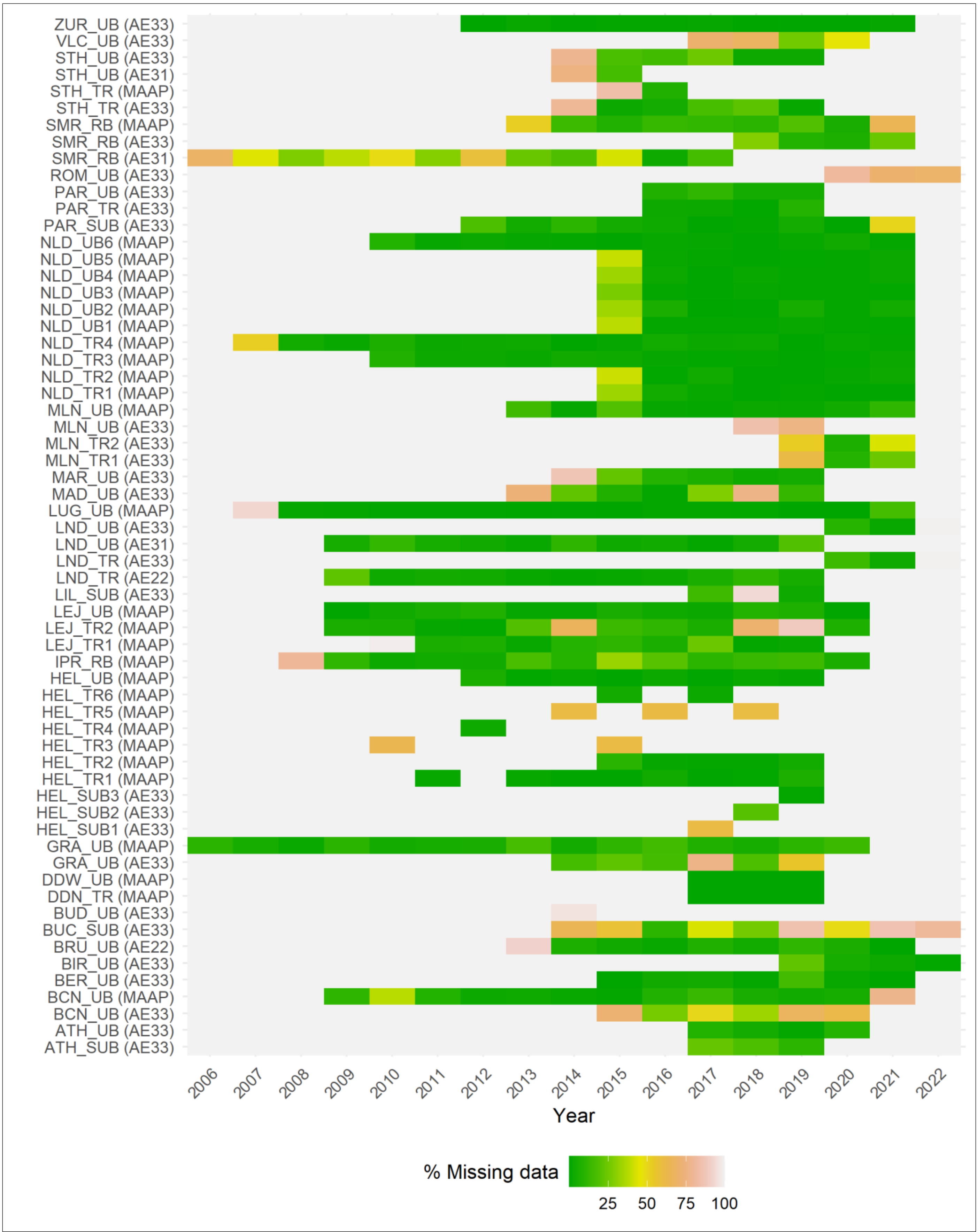

Figure S1. Complied eBC mass concentrations data converge and data capture in each year during the minimum and maximum data available ranged from 2006 to 2022 measured by MAAP or aethalometers. The blank area represents 100% missing eBC data between 2006-2020, which is either unavailable in our database or not compiled for this study. The color bar extends to the bold green area, indicating 100% data availability during that period of the year.

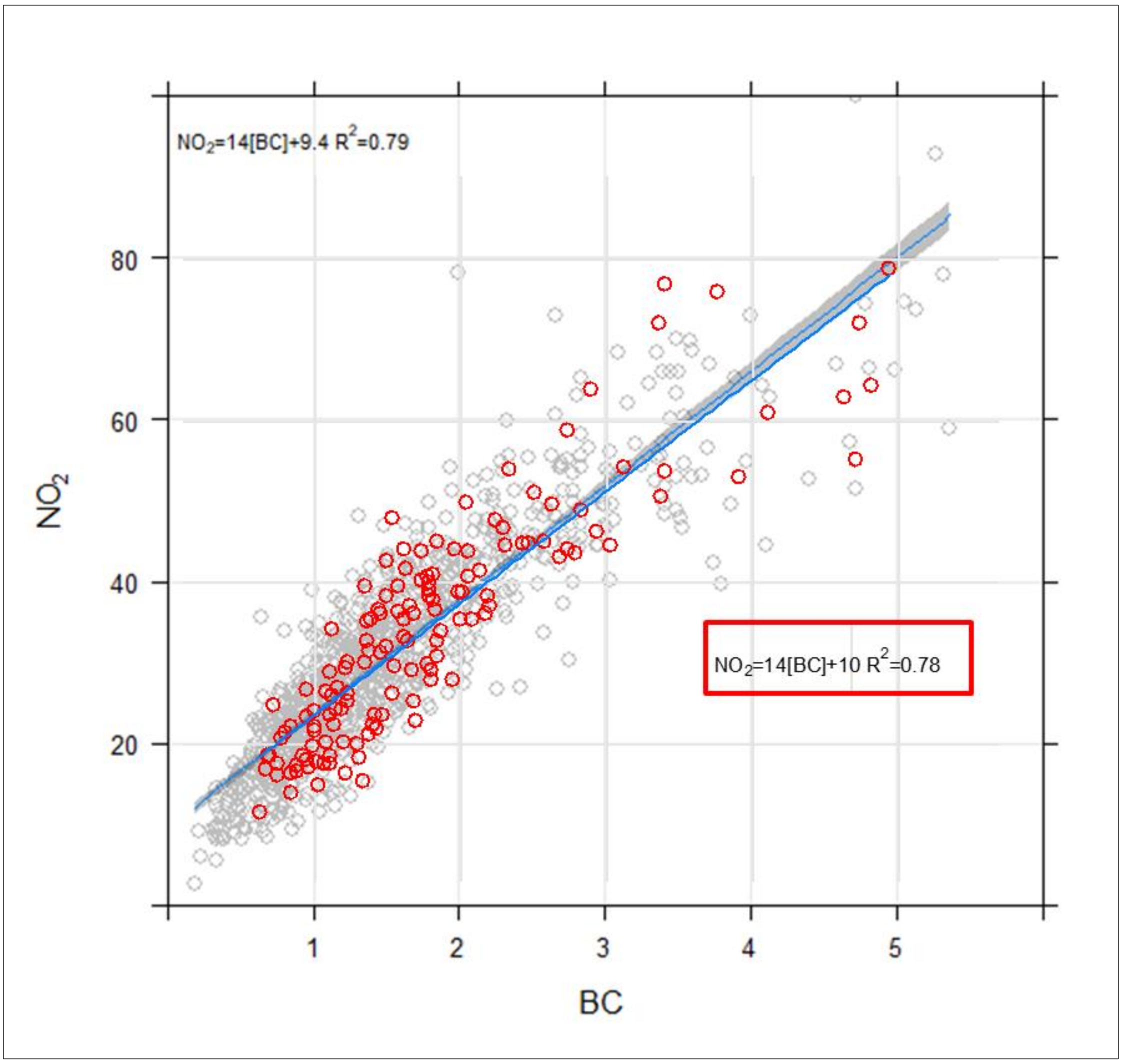

Figure S2. The relationship between eBC concentrations from MAAP and NO_2 concentrations in BCN_UB with (red circles) and without (grey circles) DDE using three years of data. Data were averaged over 24 hours., Slope, intercept and correlation coefficient are very similar indicating a non-significant effect of DDE on eBC concentrations data.

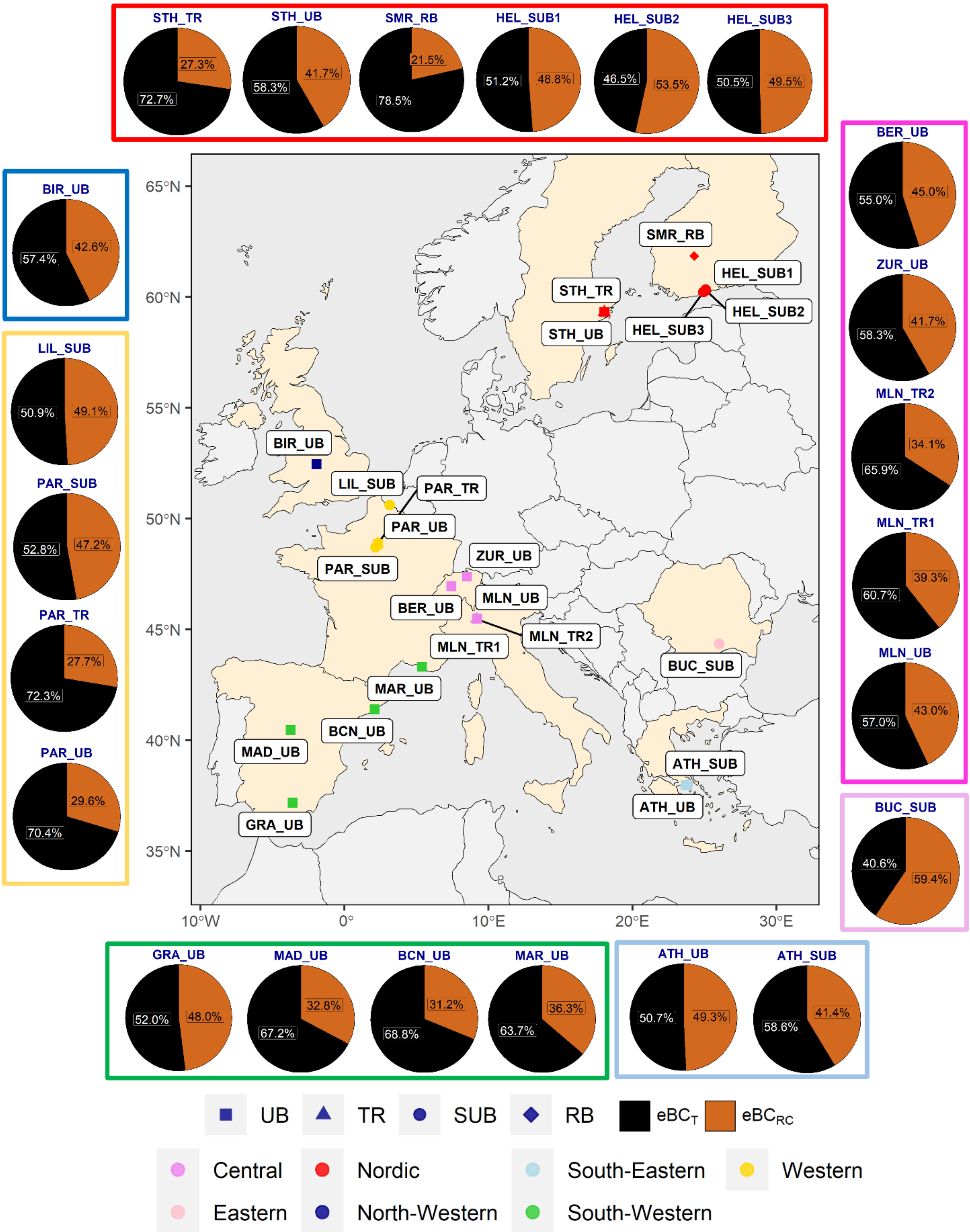

Figure S3. Source apportionment of eBC mass concentration applying aethalometer model applied for 23 sites using AE33 eBC data during the study period (2017-2019), Location of the sites and geographic regions are highlight using different colours. The results are presented based on AAE_T= 0.90, AAE_{RC}= 1.68, Zotter et al. (2017).

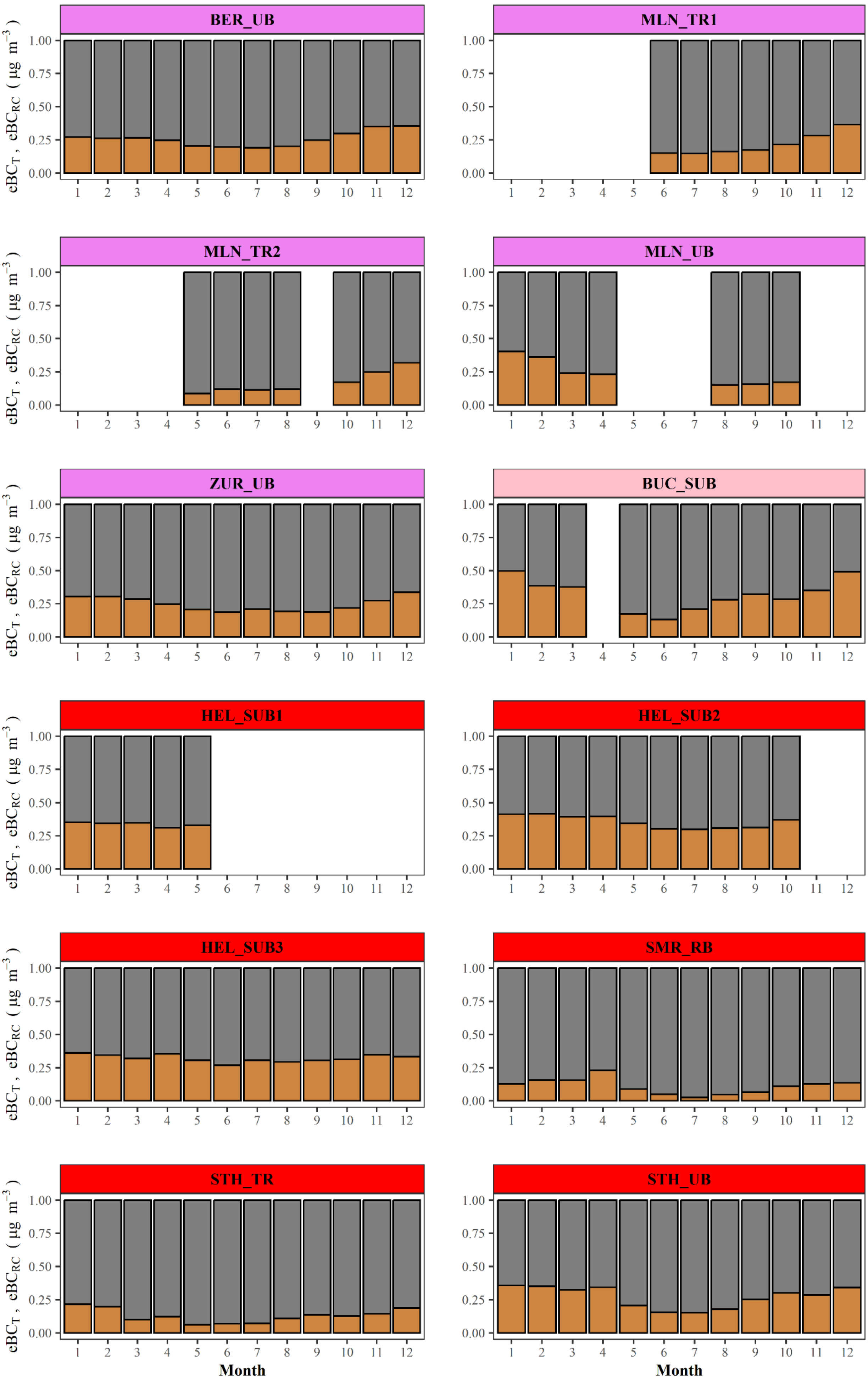
BER_UB
MLN_TR1
MLN_TR2
MLN_UB
ZUR_UB
BUC_SUB
HEL_SUB1
HEL_SUB2
HEL_SUB3
SMR_RB
STH_TR
STH_UB
eBC_T , eBC_{RC} (μg m^{-3})
1.00
0.75
0.50
0.25
0.00
1 2 3 4 5 6 7 8 9 10 11 12
Month

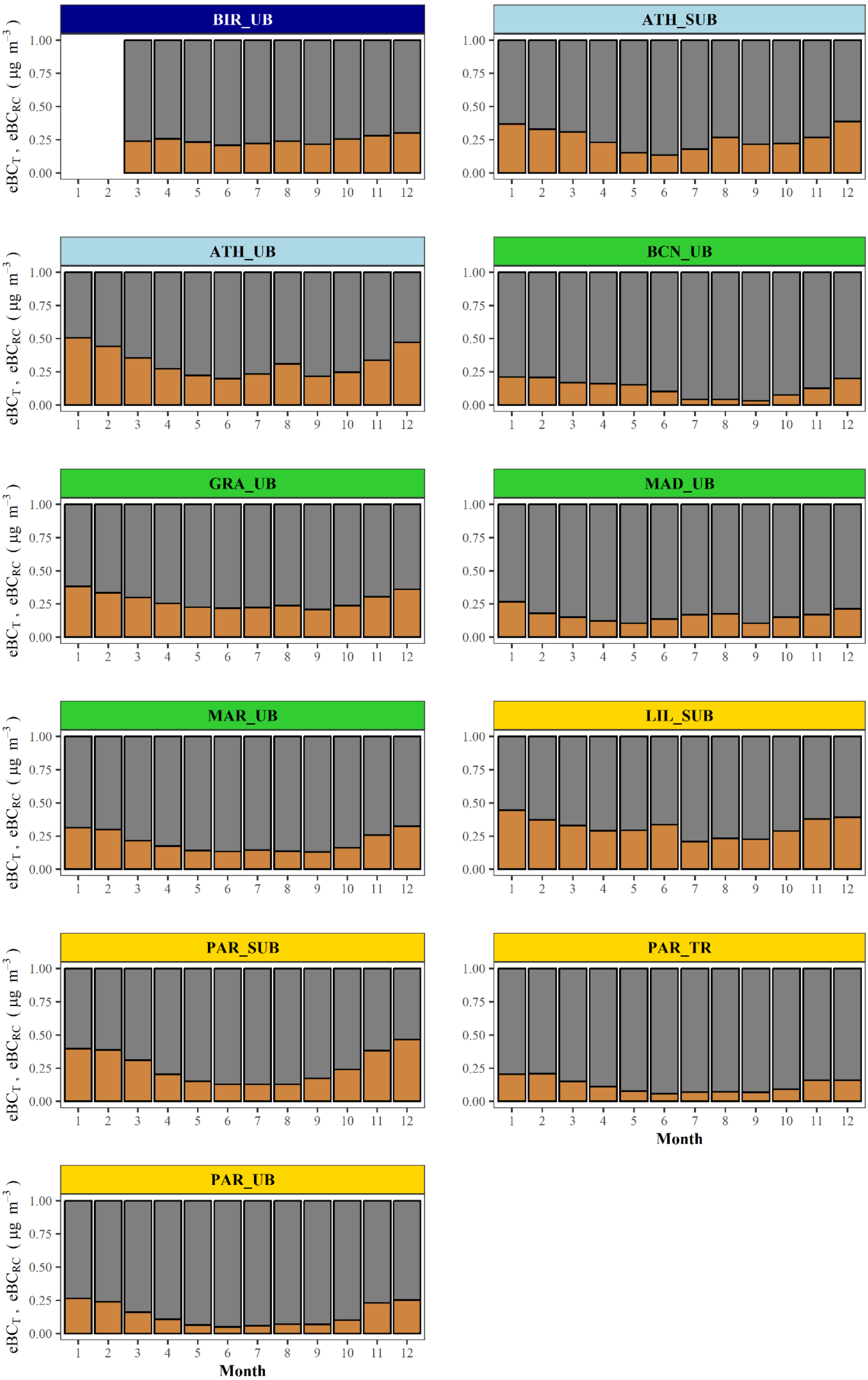

Figure S4. 100% stacked histograms of monthly variation as a result of the source contributions of eBC$_T$ and eBC$_{RC}$ through the application of the aethalometer model based on AAE$_T$= 1 AAE$_{RC}$= 2. These histograms depict the results obtained from AE33 eBC mass concentration datasets at 23 different sites. The stacked bars within each site's column represent the relative contributions of eBC$_T$ and eBC$_{RC}$

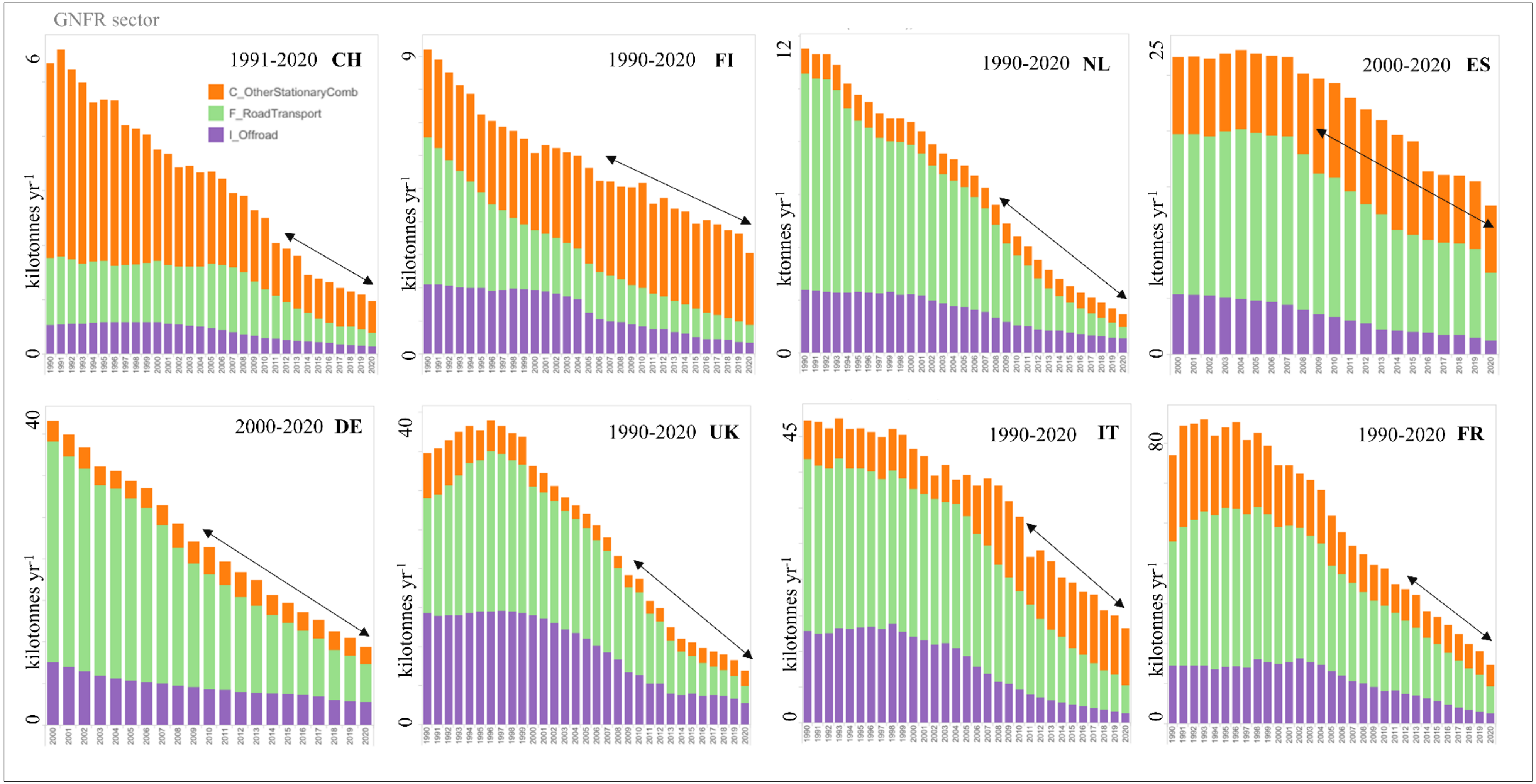

Figure S5. Official national annual emissions of BC (in kilotonnes per year) for GNFR sectors. C (Other stationary combustion, which includes residential and commercial heating), F (Road traffic), and I (Off-road), for member states included in the trend analyses of this study. Data obtained from CEIP (2023). Black arrows indicate the period of BC covered for trend analysis in the city of the respective country. The emissions from stationary combustion activities can be categorized into commercial and institutional sector, residential sector, and other stationary sectors such as agriculture, forestry, fishing, and military sectors. Pollutants mainly related to residential wood combustion processes are emitted from other stationary combustion activities. In terms of road transport emissions, the main pollutants are gasoline exhaust, diesel exhaust, liquified petroleum gas (LPG) exhaust, and non-exhaust emissions. Off-road transport includes emissions from non-road mobile machinery used in various sectors such as commercial (e.g. transportable equipment), residential (e.g. gardening and handheld equipment), agriculture, forestry and fishing (e.g. harvesters, cultivators), manufacturing industries and construction (e.g. excavators, loaders, bulldozers), and other categories such as military, land-based railways, and recreational boats. CEIP, 2023, EMEP Center for Emission Inventories and Projections. https://www.ceip.at/data-viewer-2/overview-dataviewers-2022

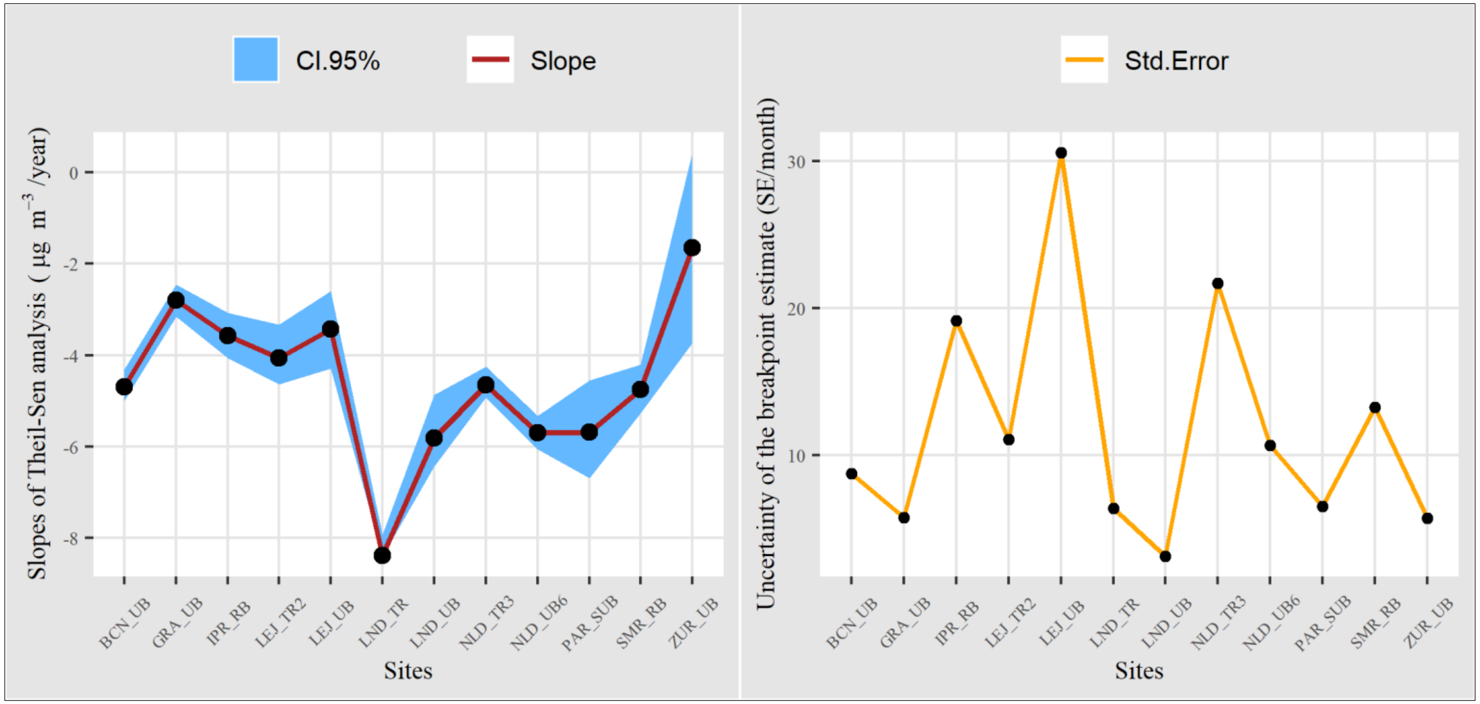

Figure S6. Slopes and corresponding confidence intervals (CI) of Theil-Sen analysis, and the standard errors (SE) of the estimated breakpoints using segmented package with piecewise regression.

References

EMEP, Centre on Emission Inventories and Projections. Data viewer - officially reported emissions data. https://www.ceip.at/data-viewer (accessed 1.30.23).

Sandradewi, J., Prévôt, A.S.H., Szidat, S., Perron, N., Alfarra, M.R., Lanz, V.A., Weingartner, E., Baltensperger, U.R.S., 2008. Using aerosol light abosrption measurements for the quantitative determination of wood burning and traffic emission contribution to particulate matter. Environ. Sci. Technol. 42, 3316–3323. https://doi.org/10.1021/es702253m

Zotter, P., Herich, H., Gysel, M., El-Haddad, I., Zhang, Y., Mocnik, G., Hüglin, C., Baltensperger, U., Szidat, S., Prévôt, A.S.H., 2017. Evaluation of the absorption Ångström exponents for traffic and wood burning in the Aethalometer-based source apportionment using radiocarbon measurements of ambient aerosol. Atmos. Chem. Phys. 17, 4229–4249. https://doi.org/10.5194/acp-17-4229-2017